

Hypersonic Morphing for the SpaceLiner Cabin Escape System

Cecilia Valluchi, Martin Sippel

Space Launcher Systems Analysis (SART), DLR, Bremen, Germany

HYPMOCES has been a Project in the frame of Research and Technological Development for Air Transport in the 7th Framework Programme 2012. The goal is to investigate and develop technologies in the area of control, structures, aerothermodynamics, mission and system analyses required to enable the use of morphing in escape systems for hypersonic transport aircrafts.

Focus is on the SpaceLiner passengers Cabin Escape System (CES). The SpaceLiner is a passenger transport system reaching hypersonic flight speeds to cover intercontinental distances in almost 90 minutes.

The CES, thanks to the implementation of morphing structures, achieves the capability to change its shape and automatically reconfigure during an abort scenario after ejection from the mother aircraft, fulfilling at the same time constraints about compactness, adaptability to the unpredicted environment and required flight performances to ensure safe landing.

A multidisciplinary design approach investigates issues related to the CES Integration within the SpaceLiner mother aircraft (DLR), GNC approaches for morphing (Deimos), Morphing Structures Design and Analysis (Aviospace), ATD-database and advanced micro-ATD analysis (ONERA).

The contributions to the HYPMOCES Project mainly concerned in this paper are about System and Morphing Structure Analyses.

Keywords: SpaceLiner, cabin escape system, hypersonic morphing, advanced material technologies.

Subscripts, Abbreviations

AEDB	Aerodynamic database
CES	Cabin Escape System
COTS	Commercial Off-The-Shelf
EMA	Electro-Mechanical Actuator
EMACU	Electro-Mechanical Actuator Control Unit
GGs	Gas Generators
I/F(s)	Interface(s)
MECO	Main Engine Cut-Off
TPS	Thermal Protection System

1. Introduction

Safety is one of the main drivers for the development of future trans-atmospheric passengers' transportation systems. The extreme thermo-mechanical environment associated to hypersonic flight as well as the high level of reliability required for the enabling technology, leads to the need of a passenger escape system to ensure safety and comfort during nominal flight and survival in case of a flight abort scenario.

The implementation of a CES within a hypersonic transport system is challenged by the integration constraints for compactness to fit within the mother aircraft structure, the limit load factors to be sustained by the passengers, the propulsion mean and related mechanisms to realize clean and quick separation, the capability to withstand the extreme thermal environment applying high-performance materials in the design and the adaptability to a wide range of abort scenarios thanks to enhanced mission flexibility through the implemented morphing structures.

Morphing refers to a change in shape to achieve adaptation to the varying flight conditions. The purpose is to enhance the aerodynamic efficiency and thus the in-flight stability in roll, pitch and yaw directions introducing additional aerodynamic surfaces. The most effective increase of the lifting body surface to affect the aerodynamic efficiency is achieved by a wing deployment, while flaps and rudders mainly improve the stability around the three body axes.

Dedicated sections describe in the following the different contributions of the partners in the HYPMOCES Project [2, 3].

2. CES Integration

The system-level activities run in DLR refer to the investigation of the integration concept for a compact combination of the morphing system within the passengers CES and of the CES within the SpaceLiner [1] mother aircraft as shown in Figure 1. A trade-off analysis to determine the best integration concept was carried out between a Baseline and a Backup Morphing Wing Concept taking into account mass, TPS layout, trim capability and system requirements with the support of an AEDB created through quick analysis tools.

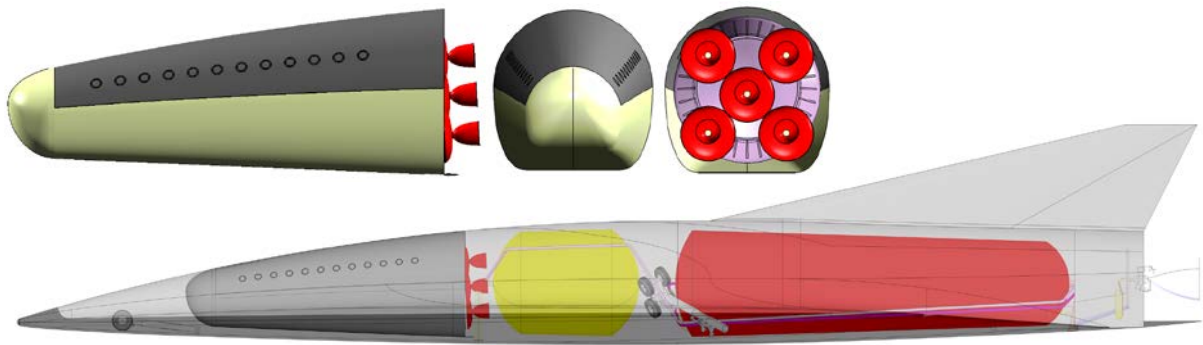


Figure 1 SpaceLiner 7 CES integration

As input for the 1st Design Loop, trajectory analyses were performed to define possible sizing abort flight points in terms of thermal and structural loads. Within an abort scenario, a case of failure occurrence leading to a catastrophic event implies the CES to be ejected from its mother aircraft followed thereafter by the deployment of the morphing wings. Potentially, an emergency capsule separation could be necessary at any point in the SpaceLiner trajectory from lift-off to landing, however the HYPMOCES Project focuses on abort scenarios occurring in the hypersonic phase of flight, see Figure 2. As a result of the investigation, the sizing flight point was defined at Main Engine Cut-Off (MECO) in which the maximum Mach number is reached because that's the flight point of maximum energy which will result in the most demanding aerothermodynamic loads.

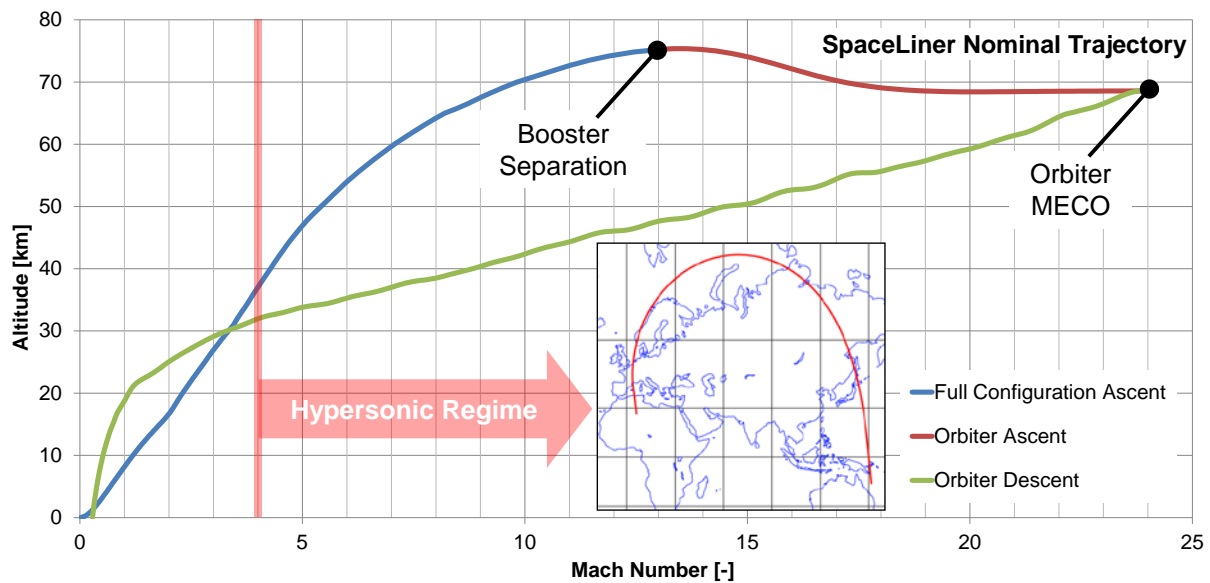


Figure 2 SpaceLiner possible abort scenarios

DLR provided from previous SpaceLiner system studies the undeployed initial CES concept. During the 1st Design Loop the Baseline and the Backup Concepts were identified.

3. Morphing Options

3.1 Baseline Morphing Wing Concept

The Baseline Morphing Wing is characterized by an inflatable structure placed on both lower sides of the CES. A multi-view of the Baseline Morphing Wing Concept is given in Figure 3.



Figure 3 Baseline Morphing Wing

The inflatable morphing wing is comprised of a flexible TPS released through bags' inflation, realized in turn by the gas generators (GGs) applied in the design. The original TPS of the capsule is cut and removed in the lower section to allow the housing of the morphing wing subsystems and in particular the deployment of the bags once inflated by the gas generators to shape the morphing wing in the deployed configuration on aerodynamic purposes as outlined in Figure 4.

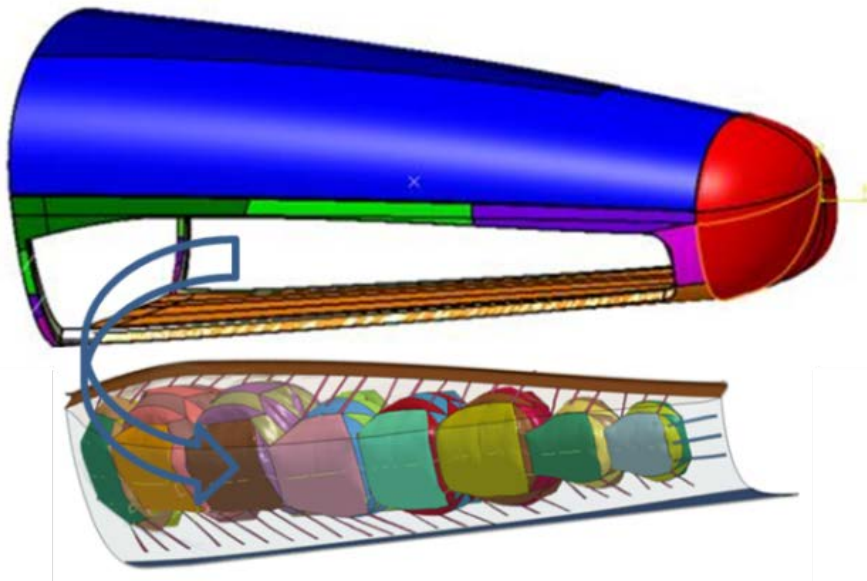


Figure 4 Original TPS cut and Baseline Morphing Wing with inflatable bags introduced

3.2 Backup Morphing Wing Concept

The Backup Morphing Wing is characterized by a particular design of a wing structure based on a hot-structure approach.

The wing is implemented, such as in the Baseline Concept, on both lower sides of the CES and is highlighted together with its deployment mechanism in Figure 5. In nominal flight condition, the wing is stowed within the CES. In case of flight abort and thus CES separation from the SpaceLiner mother aircraft, the wing is deployed by releasing preloaded springs through a hinge mechanism creating a flat envelope for the wing in-plane rotation. The capsule's original TPS is cut on purpose to match with the envelope created by the wing rotation and in order to guarantee the sealing with respect to the high-temperature incoming air and resulting heat flux during the short transient after separation, an ejectable protective tile is applied in the original TPS design.

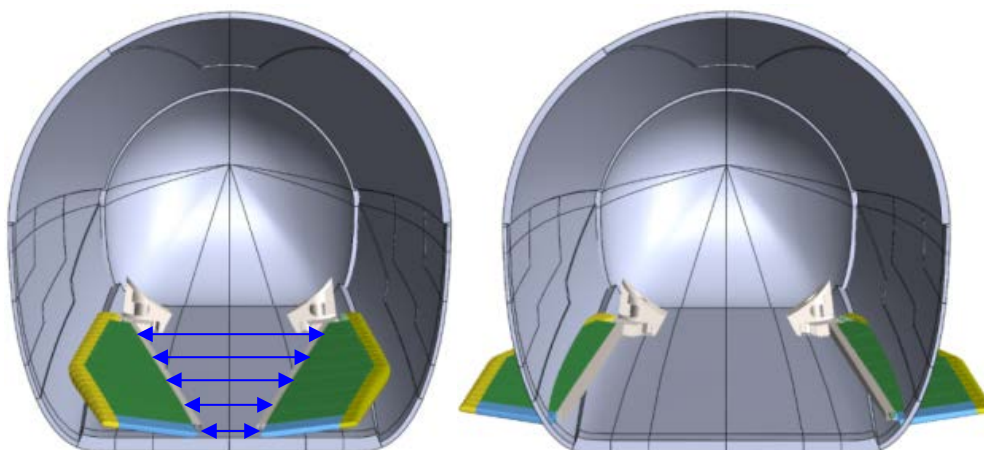


Figure 5 Backup Morphing Wing in stowed position (left) and deployed (right)

The hot-structure approach applied in the current design is based on materials capable to withstand the demanding thermo-mechanical environment of hypersonic flight, fulfilling at the same time the maximal structural efficiency with a minimal contribution in terms of weight. Suitable materials are applied in the design shown in Figure 6 as a function of the operative temperature ranges implied in

the mission profile. In particular, leading edge, windward panel and trailing edge exposed to higher heat fluxes, consist of a Ceramic Matrix Composite (CMC) material as for example C/SiC, while the internal structure and the leeward panel exposed to lower heat fluxes are made of Titanium alloy.

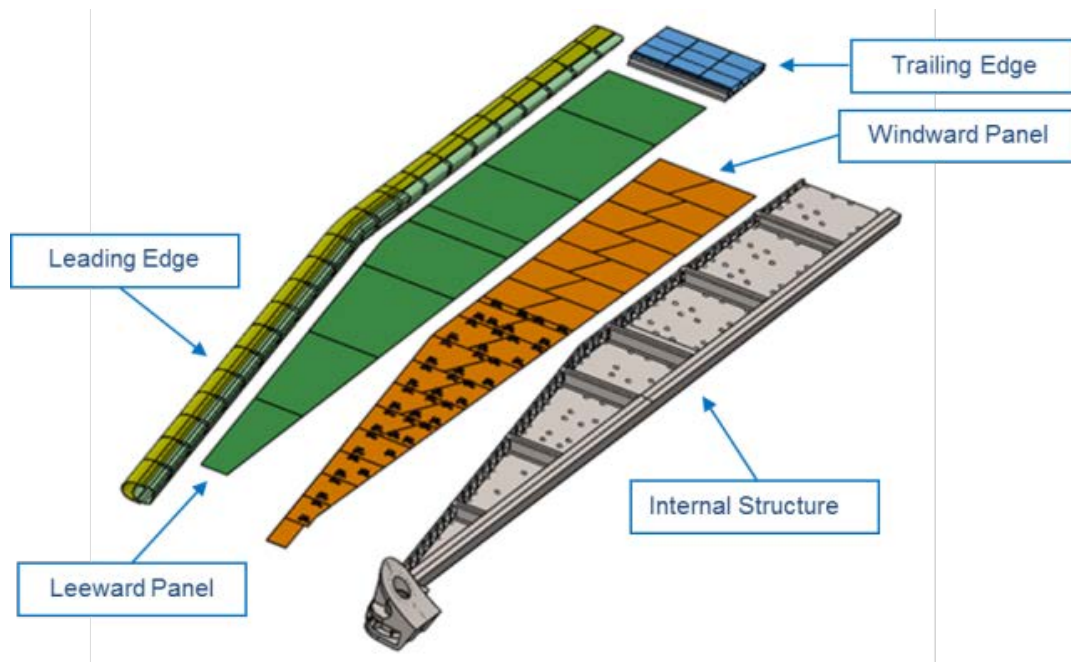


Figure 6 Structural layout of Backup Morphing Wing (Aviospace design)

3.3 Trade-Off Analysis

A multidisciplinary evaluation of the Backup and Baseline concepts has been performed identifying a set of performances as well as benefits, challenges and critical aspects for both technical solutions. Criteria are listed in Table 1. Both concepts are shown in front-view comparison in Figure 7.

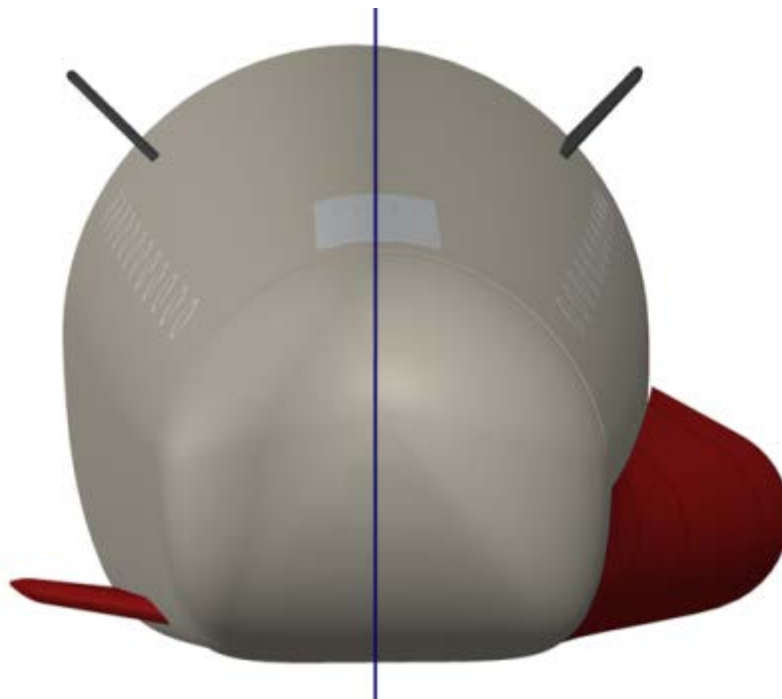


Figure 7 Backup/Baseline Concept trade-off

	BASELINE	BACKUP
→ mass contribution	<10%	12%
→ compact design in stowed configuration and impact on the original capsule design	✓	✓
→ TRL	✓	✓
→ aerodynamic performances (L/D, pitch roll and yaw static stability)	✓	✓
→ structural stability	✓	✓
→ cost	✓	✓

Table 1 Trade-off analysis between the Morphing Wing Concepts

The Baseline Concept turns out to be the best morphing wing solution to implement within the CES, mainly because of the reduced mass contribution, the better aerodynamic performances and the cost implied.

The trade-off analysis is focused on the Morphing Wing Concepts. However, the CES design comprises also additional morphing structures as rudders and flaps to enhance the capsule stability and controllability in yaw, pitch and roll directions.

4. System-level Supporting Activities

Supporting activities in the Project Design Loops in the definition of the best concept for the integration of the morphing structures within the CES were performed and are briefly discussed in the following.

4.1 Thermal Protection System Definition

The TPS of the CES protects the passengers and the allocated subsystems from the extreme thermal environment encountered during a typical SpaceLiner trajectory at hypersonic flight speeds and it is characterized by the materials' layout presented in Figure 8 and Table 2. A more detailed description has been published in reference 4.

4.2 Parachutes Characterization

Parachutes are implemented in the SpaceLiner CES to enable the deceleration and the stabilization of the passengers' capsule during the supersonic, transonic and subsonic phase of flight to landing. The parachutes are deployed and operate within a defined altitude/Mach envelope with upper limits of 24 km of altitude and Mach number of 3.

The complex aerodynamic behaviour of the CES flying through the different regimes affects the parachute system design resulting in a combination of a supersonic stabilization chute allowing a safe deceleration through the transonic phase of flight and a subsonic parafoil for gliding back to Earth.

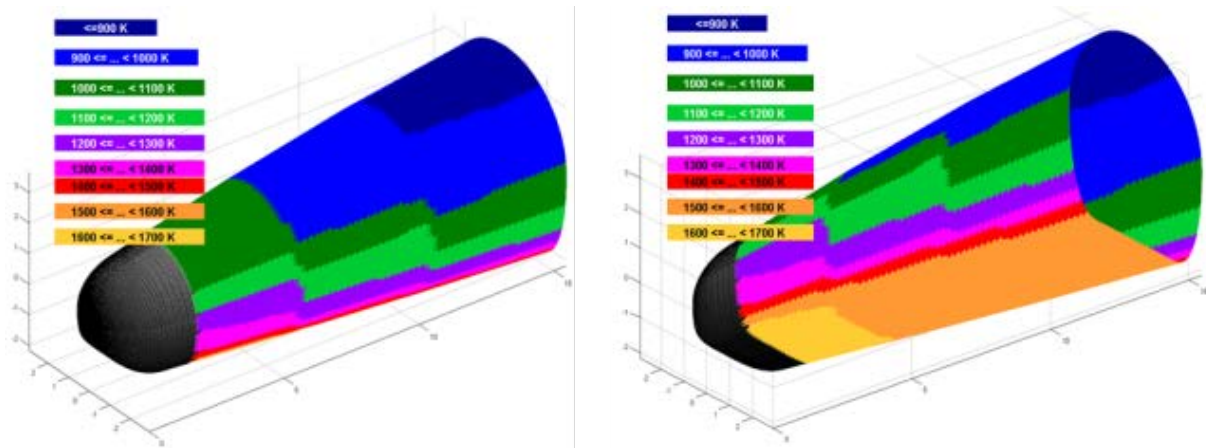


Figure 8 CES TPS-distribution as function of maximum expected temperature range [4]

Temperature [K]	Material	Thickness [m]	Mass [kg]
Nose	AVCOAT	0.133	1335
700 – 800	AFRSI	0.0885	223
800 – 1000	TABI	0.1094	864
1001 – 1100	TABI	0.0544	16.2×2
1101 – 1200	TABI	0.0551	12.6×2
1201 – 1300	TABI	0.0557	12.8×2
1301 – 1500	AETB	0.0719	9.8×2
1501 – 1850	CMC	0.1910	401×2
Total			3327

Table 2 CES TPS characterization

4.3 Bag inflation gas generators

The gas generators design is fulfilled taking into account the configuration of the bags realizing the nominal shape of the morphing wing defined by aerodynamic and structural constraints, as shown in Figure 9. Typical automotive airbag gas generators with solid propellant are to be selected.

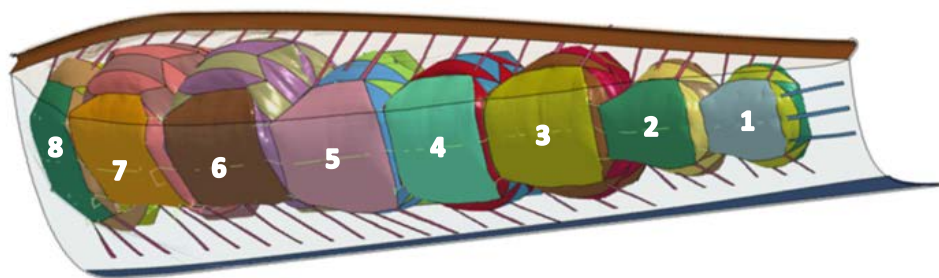


Figure 9 Deployed Morphing Wing configuration showing bags inflation by the GGs

Design requirements for bags' inflation are:

- inflation pressure of 20% above the external total pressure peak;
- inflation time less than 2 s.

Moreover, implementation of valves for the bags' internal pressure regulation for adaptation to the varying conditions of the external aero-thermodynamic are possible but have not been investigated within HYPMOCES. The very high reliability of the GGs offsets the need to implement additional casings for redundancy purposes, saving so mass and keeping the system simple.

4.4 Flaps Actuation System Sizing

Two bodyflaps are implemented in the capsule design to get pitch and roll control. The actual system design focuses on electro-mechanical actuators (EMAs) and batteries' sizing to achieve flaps' control. The flap control system architecture taking inspiration from the IXV design [5] is characterized by two electro-mechanical actuators interfacing the flap rods by two levers, an electro-mechanical actuator control unit (EMACU), a battery set and cables' harness.

The actuation system to steer the aerodynamic control surfaces is sized on the basis of input data delivered by the partners in the Project, i.e. ONERA, DMS and Aviospace, moreover components already available in the commercial marketplace (COTS) are applied in the design shown in Figure 10.

Input data are collected from ONERA about the pressure coefficient distributions on the flaps for the cases of maximum and minimum deflection in the operative range. Additional input data for the dynamic and static pressure values are supplied by DMS for the worst case of maximum dynamic pressure spread over the whole re-entry trajectory to keep a conservative approach. The flap design developed by Aviospace matches the constraints induced by the demanding thermo-mechanical environment experienced during hypersonic flight. The design is taken into account to get the relative dimensions and compute the forces acting on the control surface. Thereafter the components of the flap actuation system, not characterized yet in the actual design, are scaled with components already available on the market and assumed as reference, like in this case the IXV flap actuation system design.

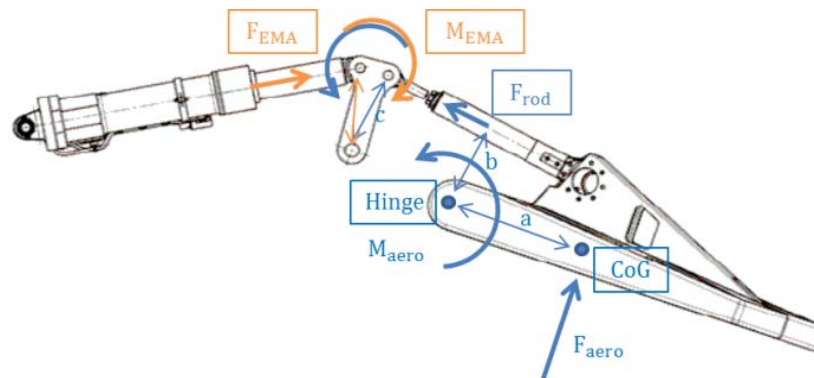


Figure 10 Flap actuator implied loads design

The power needed for electro-mechanical actuation to continuously control the flap at the maximum and minimum deflection angles is sized accounting for a given maximum rotation ω of 15°/s and the aerodynamic moment acting on the flap itself as summarized in Table 3.

	$\delta_{MAX}=+15^\circ$	$\delta_{min}=-10^\circ$
c_p	1.5	0.5
P [kN/m ²]	31.68	12.58
F_{aero} [kN]	73.5	29.19
M_{aero} [kNm]	55.86	22.18
F_{rod} [kN]	159.60	63.37
M_{EMA} [kNm]	47.88	19.01
$\omega=15^\circ/s$ (EMA sizing)		
P_{hinge} [kW]	14.64	5.81

Table 3 EMA sizing data

The maximum power required for flap actuation as a result of the previous calculation is in the amount of 14.64 kW for each flap and the outcome of a deep research about commercial off-the-shelf (COTS) highlights suitable characteristics of the VEGA P80 thrust vector control (TVC) EMA developed and qualified by SABCA.

Finally, the EMA of the VEGA P80 TVC is chosen to fit with the CES flap actuator power requirements. Relative dimensions and weight characteristics are outlined in Table 4.

VEGA P80 TVC – EMA	
Dimensions [mm]	250×350×1050
Mass [kg]	78×2

Table 4 COTS characteristics applied to the EMA design

4.5 Battery Sizing

The battery sizing is performed taking into account a power average value between the maximum and minimum flap deflection and a maximum flap rotation $\omega = 7.5^\circ/\text{s}$, whereby the energy for a total flap deflection is computed and represented in Table 5, keeping the values of the forces and moments presented in Table 3.

	$\delta_{\text{MAX}}=+15^\circ$	$\delta_{\text{min}}=-10^\circ$
$\omega=7.5^\circ/\text{s}$ (battery sizing)		
P_{hinge} [kW]	7.31	2.90
E [kJ]	17	

Table 5 Battery sizing data

According to the requirements:

- 1500 s of flight duration,
- 80% of EMAs' efficiency,
- Li-ion batteries,

the average amount of power computed in the previous analysis is about 5.105 kW for each flap and since the flight duration considered from MECO to landing is about 1500 s, the need of high energy density batteries comes to light. Therefore a battery module architecture comprised of SAFT VL8P lithium-ion cells is selected [6] as in the first three VEGA stages TVC application.

Considering the whole flight duration and an electro-mechanical actuator efficiency of 80%, the energy to be supplied by the batteries is about 2.552 kWh that for a single battery nominal energy of 100 Wh reflects in a total amount of 26 batteries for each flap. The battery architecture is characterized by overall 2 battery modules in an assembly of 13 rows and 2 strings, giving a total of 52 Li-ion cells.

The datasheet of VL8P lithium-ion cells [6] defines a weight for a single battery of 380 g, so the total mass of the battery modules is about 20 kg. No additional mass margin is considered since the batteries are in commercial use and have been successfully employed in the VEGA TVC application.

5. Morphing Structures Design & Analysis

The design and analysis of the morphing structures, namely the morphing wings, rudders and flaps, to define their thermo-mechanical architecture was part of the Aviospace team activities.

5.1 Baseline Morphing Wing

The Baseline Morphing Wing is characterized by the thermo-mechanical design of the flexible TPS and the bags inflated by means of the GGs.

5.1.1 Flexible TPS

The thermo-structural design of the flexible TPS suggests a split configuration, shown in Figure 11, in which the thicknesses of the TPS layer differ in relation to the expected heat flux on the windward and on the lee-side with the purpose of saving mass.

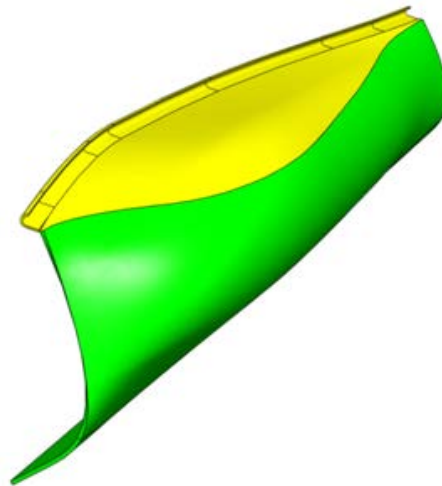


Figure 11 Flexible TPS split design

The layout of the upper (left) and lower (right) part of the flexible TPS, represented in Figure 12, are respectively characterized by a number of 13 and 17 layers, a thickness of 24 mm and 47.5 mm and a specific mass of about 10.1 kg/m² and 13.7 kg/m².

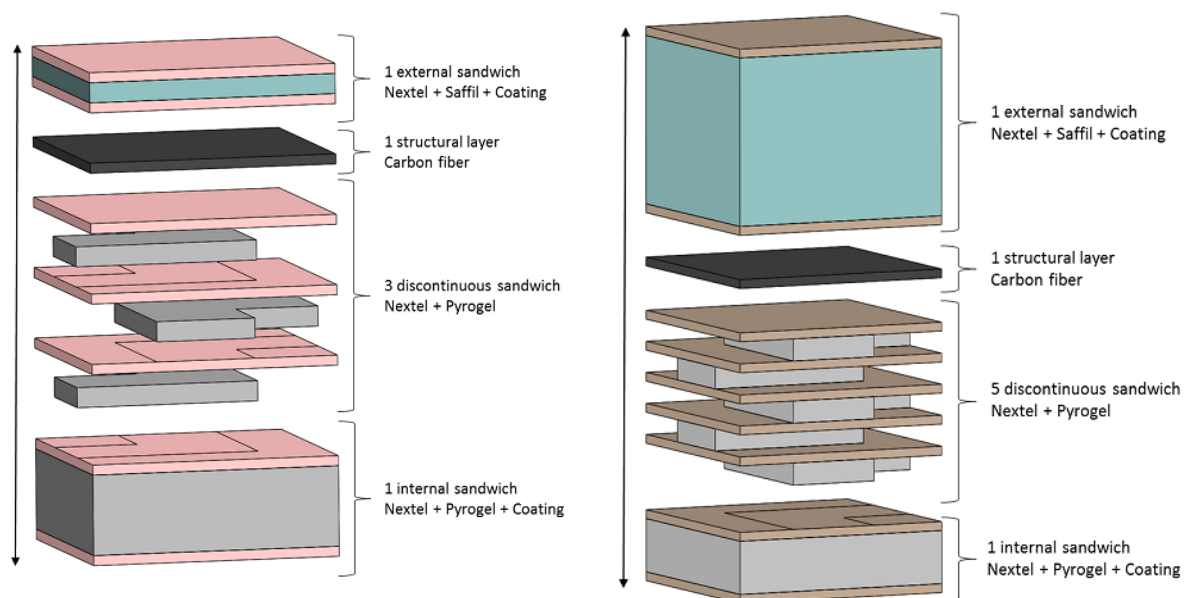


Figure 12 Flexible TPS layout of upper section (left) and lower section (right)

The thermo-mechanical analysis results for the TPS on the lower side subjected to a higher amount of heat flux are reviewed in the following Figure 13, Figure 14. The peak of the heat flux envelope

expected on the inflatable side walls in the most demanding separation condition is around 300 kW/m² [2, 3].

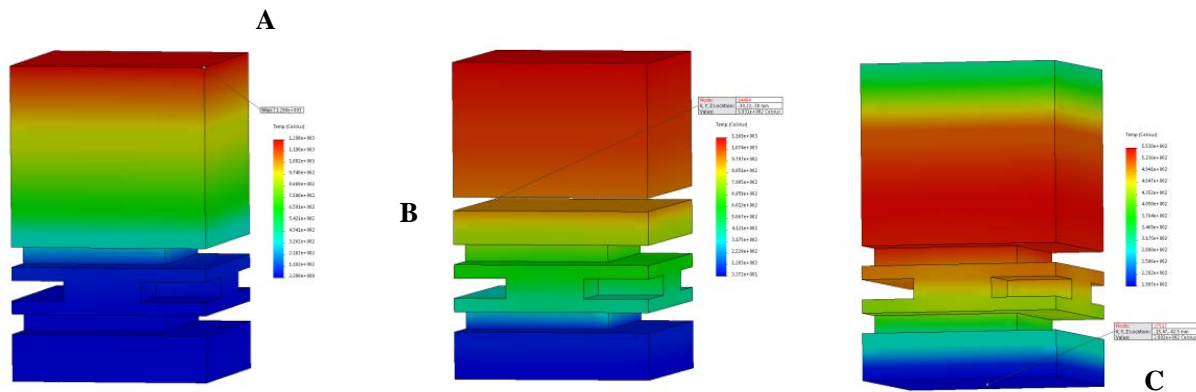


Figure 13 TPS thermal analysis results – spatial distribution for lower section flexible TPS

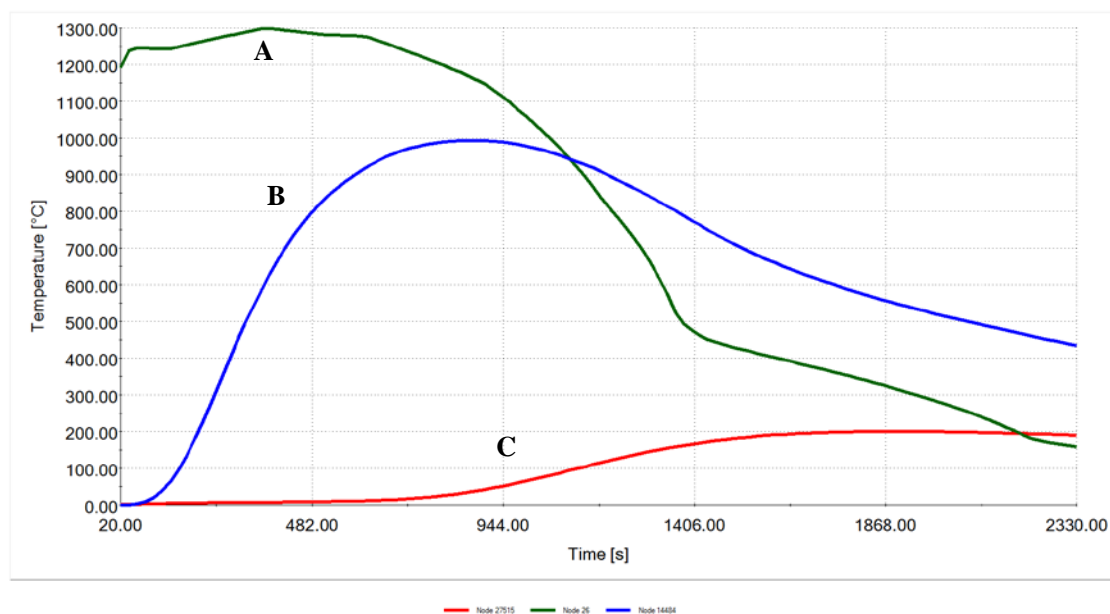


Figure 14 TPS temperature profile in time for lower section flexible TPS

The maximum temperatures reached in between different TPS layers are:

- Nextel external surface 1298 °C @ 380 s (curve A),
- Pyrogel I/F 993 °C @ 860 s (curve B),
- Nextel internal surface 200 °C @ 1880 s (curve C).

5.1.2 Inflation bags characterization

A detailed analysis of the bags inflation process which is expanding the flexible TPS into its intended shape and position has been performed. The bags are characterized by an initial folded configuration, deployed like a unidirectional telescopic bellow-structure, provided with belts and cables as reinforcements connecting the bags to each other as well as to achieve the final desired shape. The layout of the bags is a multi-layer configuration using materials like, Kapton, Zylon fabric and Dyneema ropes as reinforcement as shown in Figure 15.



Figure 15 Typical bag design for morphing wing

5.1.3 Transient simulation for bags' inflation

A full dynamic explicit simulation in the LS-Dyna environment, including multiple nonlinear effects for bags' inflation and TPS deployment, is performed through a detailed characterization of both the bags and the flexible TPS to achieve in an iterative approach the optimum shape defined by aerodynamic constraints.

The results obtained and highlighted in Figure 16, at the cost of very high CPU time (simulation is based on 690'000 deformable elements, 1'350'000 rigid elements, Physical inflation time: 3 s, Time step $\approx 3e-6$ s, CPU time @ 4 processor cores: ≈ 1 month) point out the technical feasibility of the Inflatable Morphing Wing Concept. Analyses of the simulations allow assessing the complexity related to the bags' and flexible TPS design as well as their dynamic close-fitting characterization. The current state of design shows some contact and stability issues in the simulation which require further tuning in potential further analyses.

5.2 Bodyflaps

Flaps are foreseen to ensure pitch and roll stability of the passengers' CES. Two flaps are located at the rear bottom of the capsule undergoing no configuration change between the stowed and deployed condition, being symmetrically or unsymmetrically actuated for respectively pitch and roll control.

The flap design is characterized by a hot structure approach, consisting of a C/SiC monolithic part and UHTC washers at the vehicle and actuator hinges I/Fs. The design of the internal stiffening ribs is driven by the thermo-mechanical loads induced by the high-speed hypersonic flight environment and is highlighted in Figure 17.

A transient analysis is performed applying a heat flux envelope with a peak of 800 kW/m^2 [2, 3] accounting for the worst-case scenario during a flight abort event causing the cabin escape system ejection from the mother aircraft. The extreme thermo-mechanical environment induces thermal and in turn mechanical loads and thus displacements, deformations and stresses complying with the thermo-mechanical properties of the materials applied in the design.

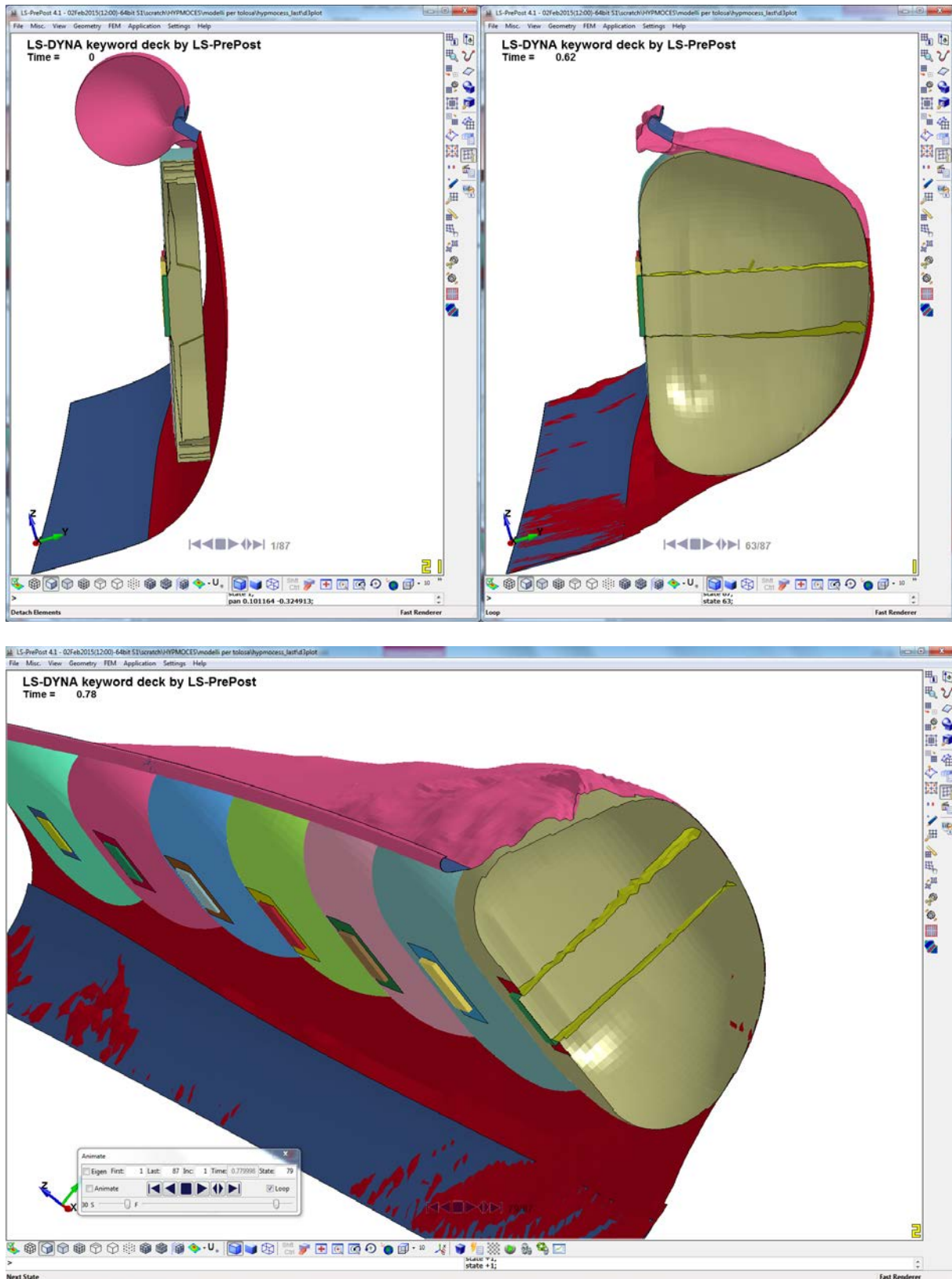


Figure 16 Bags' deployment full dynamic explicit simulation.

SI 1.7: HYPERSONICS SYSTEMS

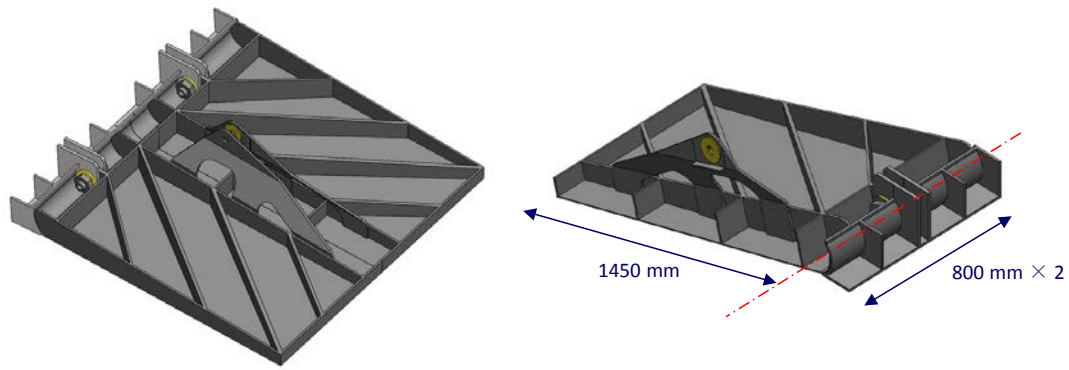


Figure 17 Flap design

In the following Figure 18 and Figure 19 the thermal analysis results of the flaps are shown in a spatial as well as representation of elapsed time.

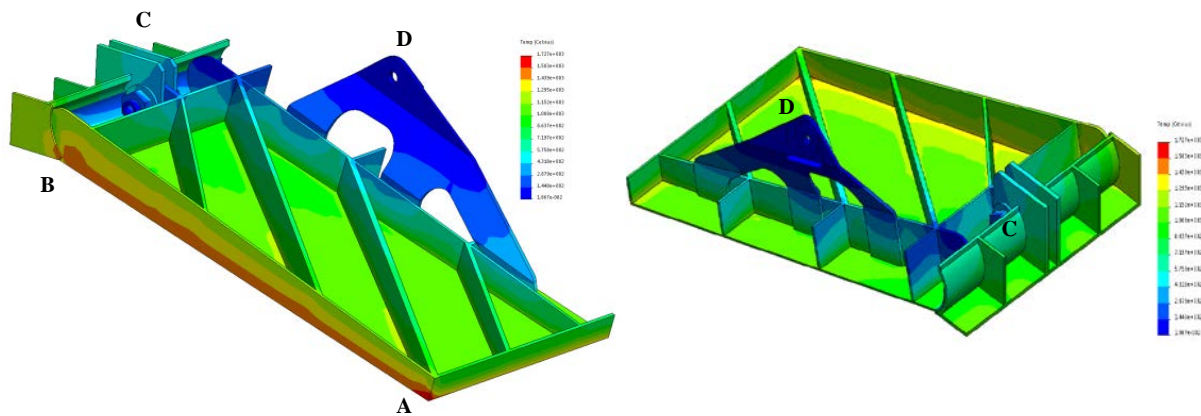


Figure 18 Flap's thermal analysis results – spatial distribution

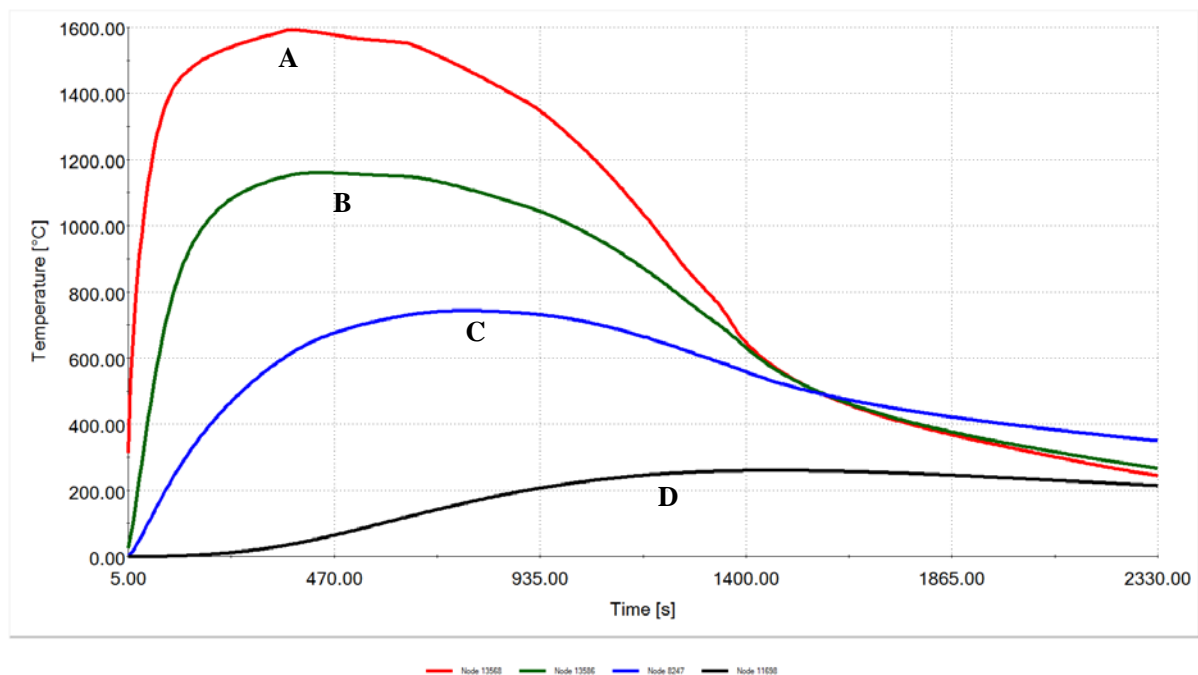


Figure 19 Temperature profile on the flap as function of flight time

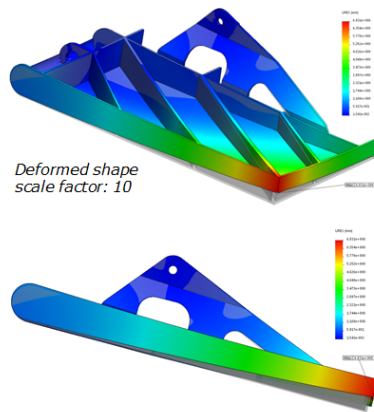
The maximum temperatures reached on the different flaps' sections are:

- Flap body: 1592 °C @ 380 s (A),
- Vehicle hinge: 743 °C @ 770 s (C),
- Actuator hinge: 261 °C @ 1470 s (D).

A linear static analysis is performed on the basis of inputs from the temperature field resulting from the previous analysis and the total external pressure as a function of time. The linear static analysis results are collected in terms of maximum deformation, maximum stress and related Margin of Safety (MoS) as highlighted in Figure 20.

STRUCTURAL ANALYSIS: Results

MAX DEFORMATION Load Case @ 50s
 P_{TOT} : 2335 Pa
 • σ (main body): 40 MPa \rightarrow MoS (1st σ) = 1,7
 • σ (hinges): 91,9 MPa \rightarrow MoS (1st σ) = 0.2
 • Δu_{MAX} : 6,9 mm



Constraints proximity

MAX STRESS Load Case @ 380 s (T_{MAX})
 P_{TOT} : 4188 Pa
 • σ (main body): 80 MPa \rightarrow MoS (1st σ) = 1
 • σ_{MAX} (hinges): 309,6 MPa \rightarrow MoS (1st σ) = -0.6
 • Δu : 6 mm

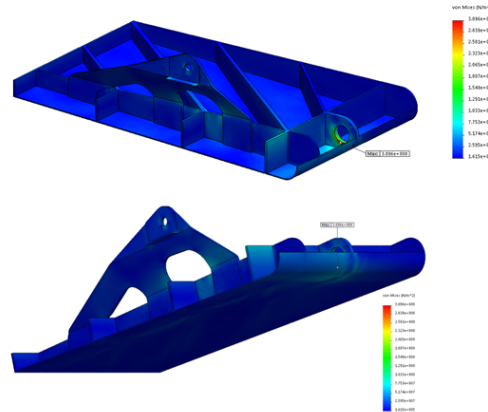


Figure 20 Flap mechanical analysis results

5.3 Rudders

Rudders are implemented in the CES design as control surfaces enhancing the yaw stability of the capsule. Two completely embedded rudders located at the rear top of the capsule are initially stowed during the nominal phase of flight and released after CES ejection through preloaded torsional springs and a locking mechanism keeping the rudders in the designed position. A pre-compressed, then released, flexible TPS is foreseen to recover the external surface continuity and achieve a smooth aerodynamic surface once the rudders are deployed.

The rudder design shown in Figure 21 is characterized by a hot structure approach as it applies to the flap. In particular, the design consists of a monolithic part of C/SiC composite material and an insulating Saffil block at the CES I/F.

The thermo-mechanical transient analyses performed assess the suitability of the optimized rudder design. Applying a heat flux envelope with a peak of 400kW/m² [2, 3] for a CES worst-case abort scenario, the resulting temperature field applied in turn together with the total external pressure in time to the structural part, induce in the frame of a mechanical analysis, displacements, deformations and stresses complying with the material properties of the structure's design.

SI 1.7: HYPERSONICS SYSTEMS

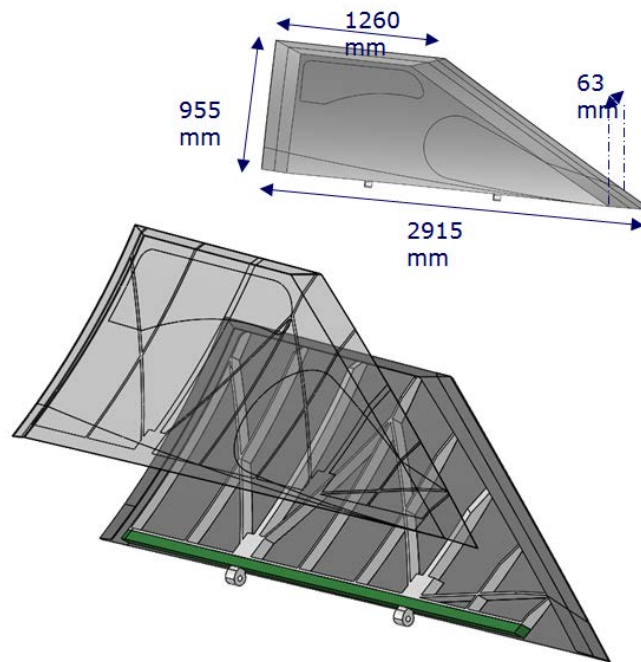


Figure 21 Rudder design

The results of the thermal analysis on the rudder highlight a temperature spatial distribution as well as a temperature profile as function of time characterized in Figure 22 and Figure 23.

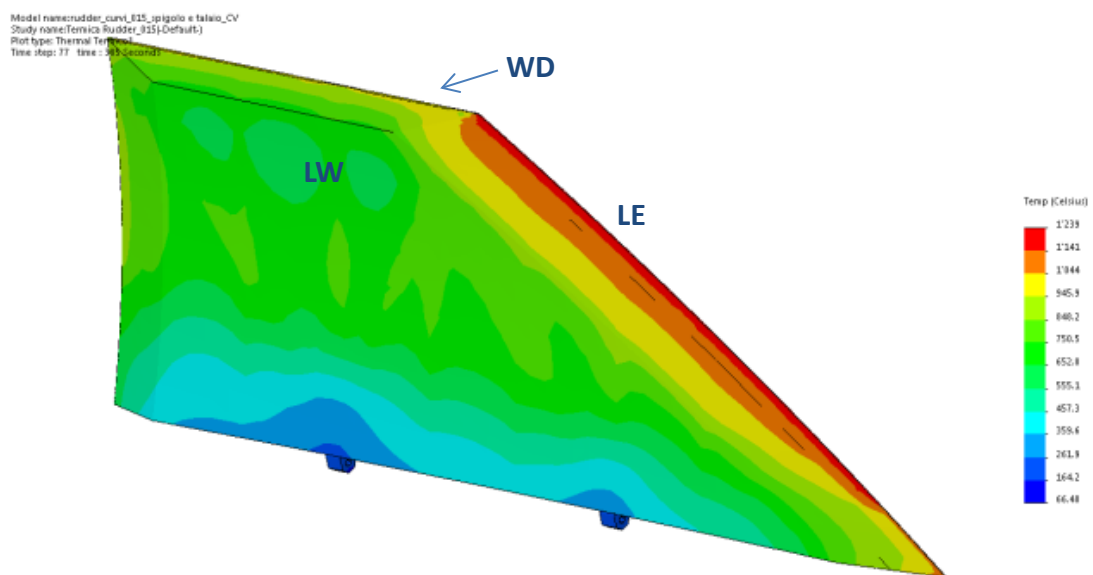


Figure 22 Rudder's thermal analysis results– spatial distribution

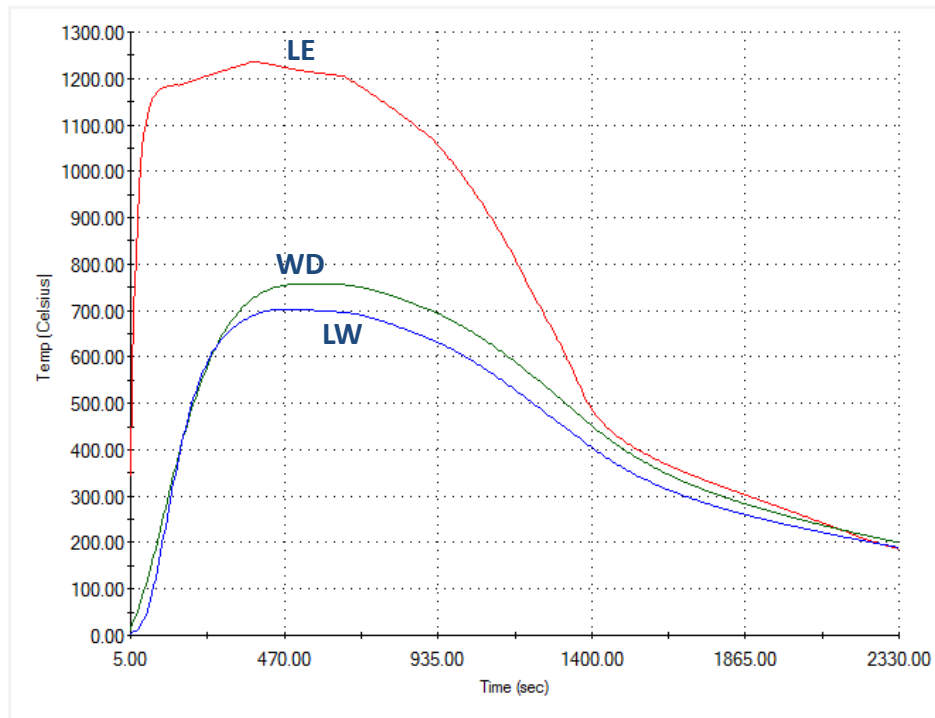


Figure 23 Temperature profile as function of time on the rudder

The maximum temperatures reached on the different sections of the rudder are:

- Leading Edge (LE) section: 1457 °C @ 380 s,
- Windward (WD) section: 1296 °C @ 385 s,
- Leeward (LW) section: 1277 °C @ 385 s.

The mechanical analysis results are summarized in the following Figure 24.

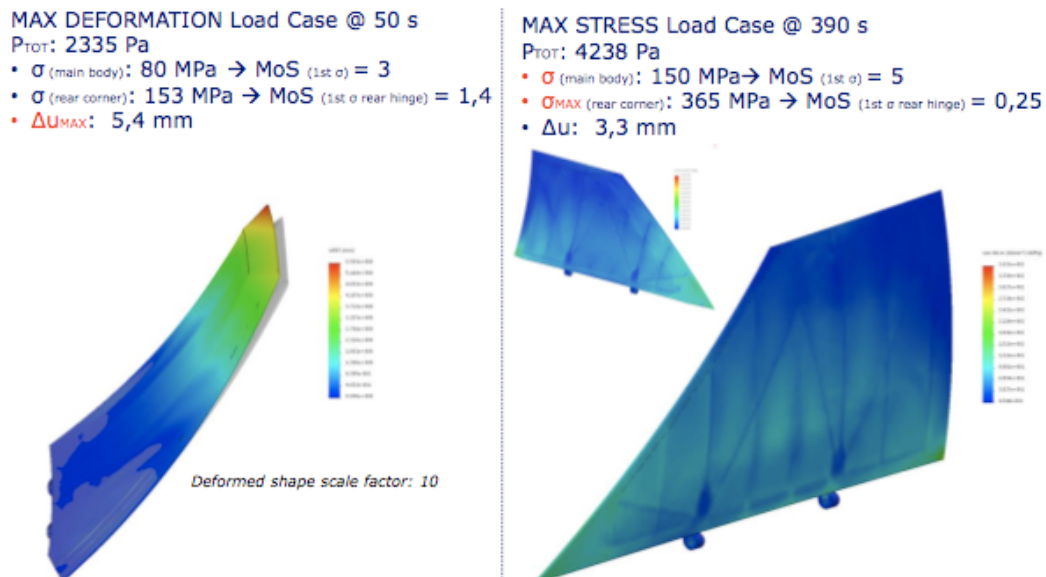


Figure 24 Rudder mechanical analysis results

6. Baseline Concept: Mass, CoG, IM characterization

The mass budget of the CES including all major components and assemblies collects the final HYPMOCES results of the multidisciplinary activities in terms of aero-thermodynamic data and thermo-structural designs.

System margins of $12 \div 14 \%$ are considered in the current design phase to keep a conservative approach on the mass estimation. The final results for both the deployed and undeployed wings in terms of mass and CoG location are reported in Table 6. The mass budget is first given for the empty stage and then for the full one with the required propellant loaded onboard, resulting in a total amount of 37 tons. The CoG of the CES is slightly affected by the change in the configuration between the undeployed and deployed morphing wings by about 5 mm in x-direction while in z-direction the offset results in a higher amount of 22 mm.

Morphing Wing	Deployed	Undeployed
Mass [kg]	30003	
Mass + Separation Motor [kg]	34183	
GLOW [kg]	37373	
CoG-x [m]	8.839	8.834
CoG-z [m]	0.467	0.489

Table 6 CES Mass and CoG characterization

The inertia matrix of the CES taking into account all the contributions of the components building up the complete system is highlighted in Table 7 and it can be noted as the pitch moment with respect to the center of mass is in the order of $1.2 \cdot 10^6 \text{ kg m}^2$.

IM_G UnDeployed_MW + Margins			IM_O UnDeployed_MW + Margins		
146972	0	-64961	154310	0	67623
0	1170114	0	0	3572908	0
-64961	0	1165563	67623	0	3561018
IM_G Deployed_MW + Margins			IM_O Deployed_MW + Margins		
156089	0	-74670	162782	0	52021
0	1178079	0	0	3582939	0
-74670	0	1180010	52021	0	3578177

Table 7 Inertia matrix properties of the undeployed and deployed morphing wing WRT the center of mass

7. Conclusions

HYPMOCES turned out to be a successful project thanks to a very effective teamwork between the partners, considering the results achieved in terms of thermo-mechanical design of the morphing structures applying a technology with a low readiness level and their implementation within a passengers' cabin escape system satisfying the strict safety requirements of manned flight and flight performances, as well as GNC approaches for morphing configurations and highly detailed aero-thermodynamic analyses.

8. Acknowledgments

The research leading to these results has received funding from the European Union's Seventh Framework Program FP7/2007-2013 under grant agreement n° ATT-2012-RTD-341531 entitled "Hypersonic Morphing for a Cabin Escape System (HYPMOCES)".

My thanks and appreciation go to the whole HYPMOCES Team, Davide Bonetti, Emmanuel Laroche and his colleagues involved in the Project but in particular to Giovanni Gambacciani for sharing his knowledge with me during my worthy work experience in Aviospace as well as for his comments to this paper.

9. References

1. Sippel, M.; Valluchi, C.; Bussler, L.; Kopp, A.; Garbers, N.; Stappert, S.; Krummen, S.; Wilken, J.: SpaceLiner Concept as Catalyst for Advanced Hypersonic Vehicles Research, 7th European Conference for Aeronautics and Space Sciences (EUCASS), Milan, 2017
2. Bonetti, D.; Sippel, M.; Laroche, E.; Gambacciani, G.: From MDO to detailed design of Hypersonic Morphing Cabin Escape Systems, 7th European Conference for Aeronautics and Space Sciences (EUCASS), Milan 2017
3. Laroche, E.; Préveraud, Y.; Vérant, J.-L. ; Sippel, M. ; Bonetti, D.: Micro-Aerothermodynamics Analysis of the SpaceLiner Cabin Escape System along Atmospheric Re-entry, 7th European Conference for Aeronautics and Space Sciences (EUCASS), Milan 2017.
4. Garbers, N.: Overall Preliminary Design of the Thermal Protection System for a Long Range Hyper-sonic Rocket-Powered Passenger Vehicle (SpaceLiner), ESA TPS-HS Workshop 2013
5. ESA Fact Sheet, "IXV: Intermediate eXperimental Vehicle", last updated 14.07.2014, http://esamultimedia.esa.int/docs/launchers/IXV_factsheet20140714.pdf (accessed October 2014)
6. Saft – Datasheet for Rechargeable Li-ion Battery Systems, VL8P